Dynamics of Alkyl Chains in Monolayer-Protected Au and Ag Clusters and Silver Thiolates: A Comprehensive Quasielastic Neutron Scattering Investigation

T. Pradeep,*,† S. Mitra,‡ A. Sreekumaran Nair,† and R. Mukhopadhyay*,‡

Department of Chemistry and Sophisticated Analytical Instrument Facility, Indian Institute of Technology, Madras, Chennai 600 036, and Solid State Physics Division, Bhabha Atomic Research Centre, Trombay, Mumbai 400 085, India

Received: October 6, 2003; In Final Form: February 19, 2004

Temperature-dependent dynamics of monolayer-protected Au and Ag nanoclusters and silver thiolates have been investigated with quasielastic neutron scattering. The simplest motion in these systems is the uniaxial rotation of the chain, which evolves slowly with temperature. While longer chain monolayers (above C_8) on Au clusters are rotationally frozen at room temperature, dynamic freedom exists in lower chain lengths. In the superlattice solids of Ag clusters, the dynamics evolve slowly, and at superlattice melting, all the chains are dynamic. The data are consistent with a structure in which the monolayers form bundles on the planes of metal clusters and such bundles interdigitate, forming the cluster assemblies. In thiolates, the dynamics is distinctly different in long- and short-chain systems. It arises abruptly at the melting temperature in C_{12} but a bit sluggishly in C_{18}, whereas in C_6 and C_8, it evolves with temperature. The data are correlated with temperature-dependent infrared spectroscopy, which preserves some of the progression bands even after the bulk melting temperature, but loses them completely above 498 K, suggesting a possible partially ordered phase in this temperature window. Our studies have established the fact that (a) no rotational freedom exists in several of the alkyl chain monolayers on metal cluster solids at room temperature, (b) simple uniaxial rotation explains the dynamics of these systems, (c) the dynamics evolves slowly, and (d) such motions arise abruptly in long-chain layered thiolates which are similar to planar thiolates. We find that longer chains can possess conformational defects at higher temperatures, which slow the rotational dynamics.

I. Introduction

Monolayers of thiols on noble metal surfaces (planar or 2D SAMs) have been the simplest of systems on which many of the fundamental properties such as friction, lubrication, etc. could be investigated.[1] They are excellent model systems, but one could use only reflection spectroscopies to study their properties.[2] In 1994 Brust et al. reported the synthesis of monolayer-protected metal clusters (MPCs) by a two-phase synthesis.[3] About 60% of the metal cluster surface was covered, whereas the coverage amounts to only 30% on planar or 2D surfaces.[3] MPCs are important in technology not only by giving a higher number density of molecules at the surface but also by preserving the nanodimension of the cluster.[4−7] Being a soluble, powdery nanomaterial, these clusters allow conventional techniques for their characterization, due to larger quantities of the monolayer surfactant, as a consequence of the high surface area (ca. 100 m^2/g).[8]

The temperature-dependent phase behavior and dynamics of molecular thin films are intimately related to their conformational order.[9] Although it is important to understand surfactancy, wetting, etc. properties, only a limited number of experimental studies have addressed the issue of phase transition of alkanethiol monolayers.[10] Recent investigations have shown that heating induces changes in the vibrational, conformational, and positional order parameters.[11,12] There have been diffraction[13,14] and scanning probe measurements,[15,16] sensitive to the spatial position of the molecule. The temperature dependence of the molecular organization and structure is important when realistic applications are considered.[17] Metal thiolate systems[18−23] are structurally similar to planar thiolates, so application of bulk techniques on them would reveal the properties of monolayers.

Each molecule of MPC has a compact, crystalline metal core. This metallic core of 1−4 nm diameter is encapsulated within a shell of tightly packed hydrocarbon chains linked to the core via sulfur atoms. Several details of the structure of the core are still unclear, but theoretical and experimental evidence suggests that it is faceted.[24−26] Electronic and optical properties are structured, showing the effects of conduction level quantization of a metallic Au^0 or Ag^0 core. From molecular dynamics (MD) simulations, we know that the equilibrium adsorption geometries of the monolayer depend on the alkyl chain length.[27−32] At low temperature, the molecules are bundled into groups with a preferential parallel intermolecular orientation of the molecular backbones in each bundle, and the bundles in turn are oriented with respect to each other.[27] The S−S distances in these clusters are 4.1 Å (on the (100) facets) and 4.3 Å (on the (111) facets). The nearest neighbor distance between Au atoms is ∼2.8 Å. These distances suggest about 12% contraction of the mean nearest neighbor distance between adsorbed sulfur atoms on a planar Au(111) surface, which results in a ∼30% increase in their packing density.[33,34] TEM and XRD measurements show

* To whom correspondence should be addressed. Fax: ++91-44-2257-0509/2545 (T.P.); ++91-22-2550-5151 (R.M.). E-mail: pradeep@iitm.ac.in (T.P.); mukhop@apsara.barc.ernet.in (R.M.).

† Indian Institute of Technology.

‡ Bhabha Atomic Research Centre.

10.1021/jp0369950 CCC: $27.50
Published on Web 05/04/2004

that the adjacent Au particles are separated by approximately one chain length, not the expected two chain lengths. This suggests that the long-range ordering arises from the interdigitation of chain domains on neighboring particles.

The structure of alkanethiolate monolayers in MPC solids has been probed in detail by ^{13}C NMR[35] and transmission IR[36−38] spectroscopies. Badia et al. compared the adsorption of thiols on a cluster surface with that of gold(I) alkanethiolates and found that the chemisorbed species on the gold nanoparticle surface is a thiolate, not a disulfide.[39,40] NMR data suggest that the long-alkyl-chain surfactant on gold nanoclusters is in a semicrystalline state. At room temperature, all-trans chains coexist with a smaller population of more mobile chains containing gauche conformers.[35] The shorter chain thiols are disordered even at room temperature. The upfield shift of the 17th carbon atom from the methyl group (C_{17}) in $C_{18}S-Au$ and the Gaussian decay of the signal in the dipolar dephasing experiments[35] suggest the presence of a motionally restricted interior of the alkyl chain and conformationally disordered chain ends. The methyl proton line widths are lower than those of crystalline alkanes, which suggest that large-amplitude motions are taking place about the chain axis.

MD simulations suggest that monolayers undergo a phase transition near the bulk melting temperature of the alkyl chain residue of the corresponding thiolate, accompanied by intramolecular conformational changes.[34] Studies predicted a first-order phase transition for both the short-chain and long-chain monolayers with the melting temperatures close to the corresponding alkyl chain melting temperature;[34] 2D SAMs of long-chain alkanethiols melt around 333 K.[41,42] The melting transition results in changes in the intermolecular structure, i.e., from the bundled state to a disordered state. The melting temperature depends on the chain length of the passivating thiol as well as the cluster core size. It has been shown that the outer boundary chains start to develop gauche defects at lower temperature than the chains near the core. At high temperature, these defects progress toward the interior, and after the melting point, both the outer and interior chains appear the same.[31] This is clear from differential scanning calorimetry (DSC)[43] and variable-temperature IR and NMR[44] measurements.

All the clusters with chain lengths of more than C_8 show a broad endotherm in DSC at 330 K, indicating a phase transition. This transition is attributed to melting of the alkyl chains. The chain melting begins at the chain terminus and propagates toward the center of the chain as the temperature increases. This result has been confirmed with FTIR and ^2H NMR studies.[44] The degree of conformational order depends on the particle size and the nature of the terminal group in addition to the chain length. Evolution of a peak at 31 ppm in the solid-state variable-temperature ^{13}C NMR spectra of C_{14} and C_{18} clusters shows a phase transition.[45] This peak is assigned to the conformationally disordered chains. As the chain length increases from C_{14} to C_{18}, the transition temperature increases from 297 to 318 K. In contrast to the long-chain samples, when the C_8S-Au sample was heated to 323 K, the only changes observed were a slight narrowing and a small upfield shift of the peaks, confirming that the short chains are already in a liquidlike state at 298 K. Deuterium NMR studies reveal that the phase transition is due to an increased frequency of the gauche conformations, caused by an increase in the free chain volume. This, in turn, results in the pseudorotational motion of the individual chain segments about the long axis of the RS chain including both axial rotation and rapid bond isomerization. From the difference in patterns of the 1,1-d_2-$C_{18}SAu$ and other samples, they concluded that there is no measurable degree of trans−gauche bond isomerization in the vicinity of the C_1-C_2 bond, and the axial rotation about the C−S bond is unlikely.

We measured variable-temperature IR of alkanethiol-protected Au and Ag clusters.[46] The d_+ and d_- (symmetric and asymmetric methyl stretching) modes show a blue shift at higher temperature. This suggests the melting of the alkyl chain. This transition appears to be reversible up to 473 K, which is confirmed by DSC. In the repeated cycles, an increase in enthalpy of this transition is observed, and is more pronounced in Ag clusters. Ex situ IR measurements[46] of the sample (after heating/cooling cycles) show the splitting of the methylene scissoring and rocking modes, which is an indication of more ordered structure.[47] This is attributed to the annealing of the monolayer on the surface. In the temperature-dependent IR spectra of monolayers on planar surfaces, the methylene scissoring mode splits in two at 80 K, which is explained as due to annealing of the monolayer.[48]

Neutron scattering is a powerful technique to study the dynamics in condensed matter, as the energy of thermal neutrons matches the energy of the excitations.[49] Taking advantage of the large cross section of protons, alkanes (hence alkanethiols) are more suitable for neutron scattering studies. In systems where there are stochastic motions, the elastic line will be broadened due to the random nature of the molecular motions, and this broadening is known as quasielastic broadening. Quasielastic neutron scattering (QENS) provides not only the time scale but also the geometry of motions. Recently, we have shown that the dynamics of the alkanethiols on Au or Ag cluster surfaces can be monitored by neutron scattering.[50] At 340 K and above, quasielastic (QE) broadening is observed in the octadecanethiol-protected Au clusters, which is explained as due to the melting of the alkyl chain.[50] It has been found that the principal rotational motion of the chains is the uniaxial motion, and the observed dynamics can be well represented with 6-fold jump diffusion.[50] This study suggests that the alkyl chains are held rigidly and the interchain distance is 4.4 Å, suggesting closest packing of chains, resulting in larger coverage than the planar monolayers.

In our subsequent work, we have shown that long-chain-thiolate-protected clusters such as AuODT ($Au-SC_{18}H_{37}$) are rotationally frozen at room temperature (RT) in a wide time scale of 10^{-9} to 10^{-12} s.[51] The *rotator* phase is absent at RT even in much smaller chain length systems, AuOT ($Au-SC_8H_{17}$) and AuHT ($Au-SC_6H_{13}$). The dynamics sets in gradually upon an increase in temperature. Alkyl chains in a metal cluster superlattice such as AgODT ($Ag-SC_{18}H_{37}$) are also dynamically frozen at RT in the whole time scale range.[51] Evolution of the dynamics with temperature is found to be different in the superlattice and isolated cluster systems. In the former, the chains participating in the intercluster interaction were found to be dynamically different from those without. On heating just above the chain melting temperature (T_{cm}), those not involved in the intercluster interaction become dynamic first. Other chains start softening subsequently, and on increasing the temperature near the superlattice melting, all the chains eventually become dynamic. The uniaxial diffusion motion about the chain axis consistently described the dynamics of the monolayers, both in isolated cluster and in superlattice systems.[52]

In this work, we have investigated metal cluster monolayers and thiolates with varying chain lengths. This is an attempt to consolidate the data over a range of systems in the context of results we have published already so that a comprehensive picture of the dynamics of these systems is obtained. The study

is consistent with previous reports, but brings out several new features and some surprises. This is true in silver thiolates as well as in metal clusters.

The paper is structured as follows. After the introduction, in section II we present the experimental methods followed by results in section III and discussion in section IV. We conclude by giving a summary of the dynamics of monolayers based on neutron scattering data.

II. Experimental Section

Samples and Methods. The preparation and characterization of these nanosystems have been discussed previously.[53] Thiolates have been synthesized as per the method discussed.[22] The metal clusters are characterized by various spectroscopies, diffraction, and microscopy.[53] Thiolates have been characterized by spectroscopy and diffraction.[18−22] The phase behavior of the systems has been studied by DSC using a Netsch DSC 4000. Variable-temperature IR spectroscopy was done with a Perkin-Elmer Spectrum One spectrometer and a home-built variable-temperature sample cell. More details can be obtained from our earlier papers.[46,53,54]

The experimental methodology for QENS has been presented in an earlier paper.[50] Briefly, the experiments were carried out using a medium-resolution quasielastic spectrometer at the Dhruva reactor in Trombay.[55] The spectrometer has an energy resolution of 200 μeV with an incident neutron energy of 5.1 meV. The quasielastic spectra were recorded in the wave vector transfer (Q) range of 0.8−1.8 Å^{-1}. The sample, contained in a sachet of aluminum foil of ∼1 mm thickness was placed at an angle bisecting the incident and the scattered beams. The sample thickness was chosen to minimize the multiple scattering effects. Measurements were carried out at different temperatures in the range of 300−400 K. The temperature measurement was accurate within ±2 K.

The systems to be discussed are octadecanethiolate ($C_{18}H_{37}S-$), dodecanethiolate ($C_{12}H_{25}S-$), octanethiolate ($C_8H_{17}S-$), and hexanethiolate ($C_6H_{13}S-$) stabilized gold clusters (AuODT, AuDDT, AuOT, and AuHT) of 3 ± 1.0 nm core diameter. We also investigated the corresponding Ag systems (of 4 ± 0.5 nm core diameter) named AgODT, AgDDT, AgOT, and AgHT. The Ag systems form three-dimensional superlattices.[53] In a superlattice system, the neighboring clusters are anchored to the lattice points as a result of the interdigitation of the monolayer chains. We have also studied the corresponding silver thiolate systems, which form planar two-dimensional structures.

In the case of the thiolate structure, the alkyl chains can have only uniaxial rotation as a result of the restriction imposed by the structure (Figure 1). This situation is quite similar to that of planar SAMs (Figure 1), except that in the latter the monolayers are stacked at an angle. In MPCs, the monolayers assemble on the surfaces of each cluster and there is indeed a possibility of two kinds of motions, both uniaxial rotation (Figure 1) and precessional motion[50] (not shown). Precessional motion requires about 5 times more energy than uniaxial rotation, as a moment of inertia calculation would predict, and therefore, uniaxial rotation should be the simplest of rotational motions possible. The hydrogens in both cases are attached to the alkyl chains, and the alkyl chains are attached to the metal. Therefore, no translational motion of hydrogen atoms is expected. The observed QENS spectra should then correspond only to the rotational motion of the hydrogen atoms about some axes, although the QENS data are not definitive on the atomic location at which rotational motion commences.

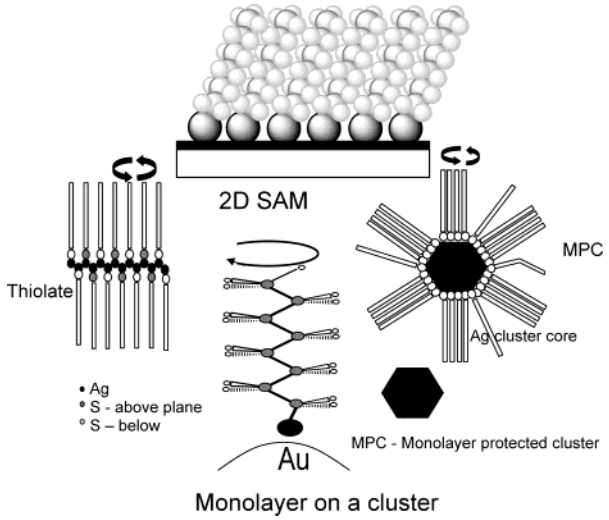

Figure 1. Schematic representation of the systems under investigation. The 2D SAM represents an assembly of monolayers on a thin metal film deposited on a suitable substrate. This resembles the thiolates. A schematic representation of an MPC is also shown. The alkyl chains, shown as rectangles, assemble on the cluster surface. Uniaxial rotational motion of the chain is shown.

The incoherent scattering law, for the rotational motion of hydrogen atoms, can be described as

$$S(Q,\omega) = A(Q)\,\delta(\omega) + (1 - A(Q))L(\omega,\Gamma(Q)) \qquad (1)$$

where the first term is the elastic part and the second term is the quasielastic part. $L(\Gamma,\omega)$ is a Lorentzian function, $L(\Gamma,\omega) = (1/\pi)(\Gamma/(\Gamma^2 + \omega^2))$, and Γ is the half-width at half-maximum (hwhm). Γ is inversely proportional to the characteristic time, τ, of the motion. It is convenient to analyze the data in terms of the elastic incoherent structure factor (EISF), which provides information about the geometry of the molecular motions. The EISF is defined as

$$\mathrm{EISF} = \frac{I_{\mathrm{el}}(Q)}{I_{\mathrm{el}}(Q) + I_{\mathrm{qe}}(Q)} \qquad (2)$$

where $I_{\mathrm{el}}(Q)$ and $I_{\mathrm{qe}}(Q)$ are the elastic and quasielastic intensities, respectively. $A(Q)$ in eq 1 is therefore nothing but the EISF. Analysis of the QENS data involves convolution of the scattering law with the instrumental resolution function and determination of different parameters ($A(Q)$ and τ) by least-squares fitting. Raw data have been corrected for crystal reflectivity, detector efficiency, detailed balance, etc. The empty sample cell background was measured and subtracted from the data. The background from other sources was taken into account by using it as a parameter and was found to be very small, almost negligible.

III. Results

Isolated Monolayer-Protected Gold Clusters. Gold clusters with different alkyl chain lengths studied through QENS techniques are AuC_6 (AuHT), AuC_8 (AuOT), AuC_{12} (AuDDT), and AuC_{18} (AuODT) (C_n corresponds to the chain length of the thiol used). First, the elastic and QE components were separated using eq 1 and were analyzed assuming possible models. Separated elastic and quasielastic components as obtained for AuHT are shown in Figure 2. No significant QE broadening was observed below 325 K in AuHT. The variations of EISF with Q at different temperatures in the case of AuHT are shown in Figure 3. It is clear that the EISF changes with

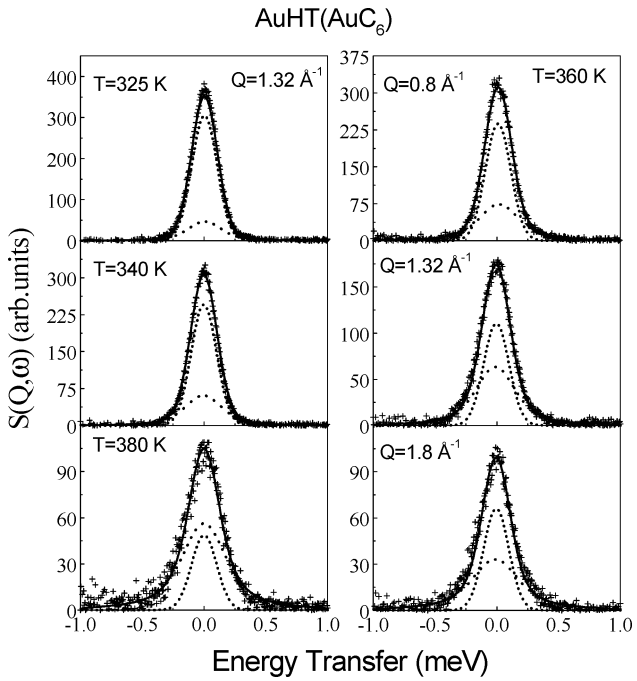

Figure 2. Typical QENS spectra and separated elastic (dotted) and quasielastic (dashed) components for AuHT at different temperatures at $Q = 1.32$ Å^{-1} and also at different Q values at $T = 360$ K.

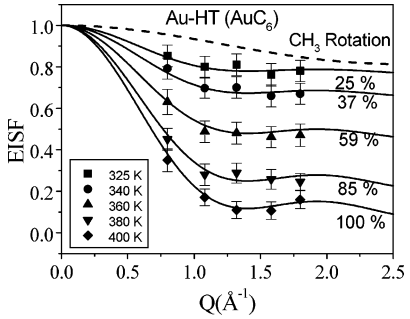

Figure 3. Variation of EISF with Q at different temperatures for AuHT. The dashed line is the calculated EISF assuming rotation of the CH_3 group alone. Solid lines are the fits using eq 4. The proportions of the protons contributing to the dynamics are indicated at each temperature.

temperature, which suggests that the geometry of rotation is different at different temperatures. Since EISF is the measure of the elastic component in the total spectrum, a large EISF means less quasielastic component, which may imply that the contribution to the dynamics is less and vice versa.

As done in our previous paper,[50] the larger EISF was explained by introducing a parameter signifying the proportion of chains not contributing to the dynamics. It has been assumed that the chains undergo uniaxial rotational diffusion. The isotropic rotational diffusion model was not considered since the alkyl chains sitting on the surface of the metal core are not expected to have isotropic rotation, and the uniaxial rotational diffusion model was found to describe the observed data.[50] It is always possible that the model could be different. If p_x is the fraction of alkyl chains in the system participating in the dynamics, then the generalized scattering law can be written as

$$S(Q,\omega) = (1 - p_x)\delta(\omega) + p_x[A_0\delta(\omega) + (1 - A_0)L(\omega,\Gamma)] \quad (3)$$

A_0 is the EISF as described above and will depend on the model. The first term on the right-hand side is the elastic contribution from the static hydrogen atoms (not contributing to the observed dynamics) in the total spectrum, whereas the second term is weighted with the fraction of hydrogen atoms in the alkyl chains participating in rotational motion. The total elastic fraction can be written as

$$\mathrm{EISF}_{\mathrm{tot}} = [p_x A_0 + (1 - p_x)] \quad (4)$$

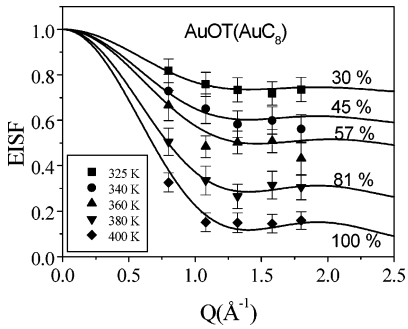

Figure 4. Variation of EISF with Q at different temperatures for AuOT. Solid lines are the fits using eq 4. The proportions of the protons contributing to the dynamics are indicated at each temperature.

Assuming the model of uniaxial rotation or jump diffusion among $N = 6$ equivalent sites, we attempted to determine p_x by least-squares fitting of the extracted EISF from the experimental data using eq 4. It may be noted that the EISF also depends on the radius of gyration and was kept as a parameter in the least-squares fit. In Figure 3, solid lines are the fits with eq 4 and the value of p_x is written below each fitted line. The calculated EISF assuming rotation of the CH_3 group alone, existing at the end point of the alkyl chain, which is expected to be dynamically active first within a whole chain, is also shown in Figure 3. A top to bottom melting model would predict such a possibility. It is apparent that the data at 325 K where the dynamics is first manifested is not describable by the CH_3 group rotation. It is seen that the proportion of alkyl chains participating in the dynamics increases with the increase of temperature. At 400 K, $p_x = 1$ describes the data very well, suggesting that all the alkyl chains take part in the dynamics.

For AuOT the variation of EISF with Q at different temperatures is shown in Figure 4. Solid lines are the fit with eq 4. The absence of quasielastic broadening at room temperature suggests no alkyl chain is participating in the dynamics. As the temperature increases, the proportion of alkyl chains participating in the dynamics increases, and at 400 K all the chains participate in the dynamics.

In the case of AuODT, no quasielastic broadening was observed till the chain melting temperature, suggesting the absence of dynamics. This was reported earlier (ref 50). The data show QE broadening above 340 K (the chain melting temperature), indicating the presence of mobile chains, and analysis shows that it corresponds to whole chain motion. The absence of the rotator phase was confirmed using a high-resolution instrument, LAM80-ET at KENS, KEK, Japan. Combining the results obtained with two instruments, it was proved that the rotator phase was absent in the wide dynamical window of 10^{-9} to 10^{-12} s.[51]

However, for AuDDT the story is quite different. On one hand, no quasielastic broadening is seen below 325 K, and on the other hand, data above 325 K indicate no elastic contribution. The absence of an elastic contribution suggests melting of the sample. This latter feature is unique within the Au cluster system, observed only for AuDDT. At 325 K it is found that about 70% of the chains contribute to the dynamics. Figure 5 shows the variation of EISF with Q. From the EISF analysis it is found that the alkyl chains in Au clusters follow uniaxial

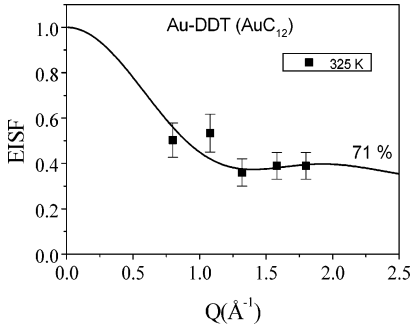

Figure 5. Variation of EISF with Q for AuDDT at 325 K. The solid line is the fit using eq 4. Data at 340 K showed a melt sample (i.e., EISF = 0). The proportion of the protons contributing to the dynamics is also indicated.

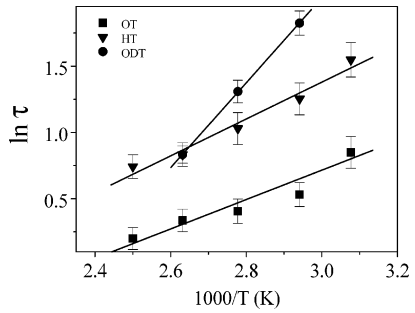

Figure 6. Variation of reorientation time for the alkyl chain in Au cluster MPC systems with temperature. The lines are the fits assuming the Arrhenius law.

rotational diffusion. Therefore, we used the scattering law corresponding to the uniaxial rotational diffusion model to fit the measured QENS spectra. Data at all the Q values and at all temperatures are well in accord. A plot of the reorientation time, τ, with $1/T$ is given in Figure 6. The small-chain systems (HT and OT) behave similarly. The activation energies for AuHT and AuOT obtained using the Arrhenius law are 2.2 (±0.3) and 2.7 (±0.3) kcal/mol, respectively, whereas for the long-chain system (AuODT) the value was 6.3 (±0.2) kcal/mol. The dynamical behavior for the intermediate-chain-length system (AuDDT) is very different. The activation energies are consistent with the chain length. A large chain length requires more energy for rotation.

Superlattice Systems. MPCs with Ag clusters form superlattice structures by virtue of the interdigitation of the neighboring chains. In the category of superlattice MPC systems, we studied AgC_6 (AuHT), AgC_8 (AuOT), AgC_{12} (AgDDT), and AgC_{18} (AgODT). In AgHT (with the smallest chain), no quasielastic broadening is seen at room temperature. But with an increase in temperature, the quasielastic component builds up, indicating an increased contribution from the dynamic alkyl chains. As described before, elastic and quasielastic components were separated in the total spectra to estimate the EISF. The variation of EISF with Q at different temperatures is shown in Figure 7; also shown is the theoretical model assuming uniaxial rotational diffusion (eq 4). The proportion of the mobile chain as obtained from the fit of the measured EISF is indicated in the figure. It is found that at 325 K only 15% of the chains are dynamic. The behavior of the EISF could not be explained by the end chain CH_3 group rotation, which in fact is expected to be dynamic at the first instant. The dynamical component increases with temperature, and finally all the chains are dynamic at 400 K, which is, anyway, the superlattice melting point. In the case of the next longer chain system, AgOT, QE broadening was observed even at 300 K. Analysis showed that

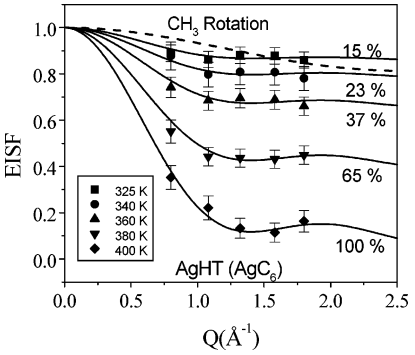

Figure 7. Variation of EISF with Q at different temperatures for AgHT. The dashed line is the calculated EISF assuming rotation of the CH_3 group alone. Solid lines are the fits using eq 4. The proportion of the protons contributing to the dynamics is indicated at each temperature.

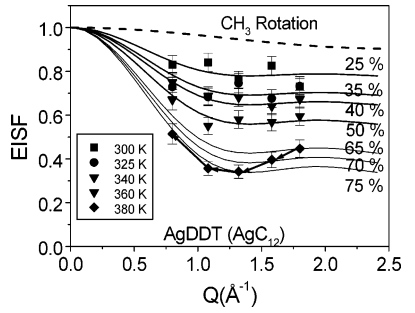

Figure 8. Variation of EISF with Q at different temperatures for AgDDT. The dashed line is the calculated EISF assuming rotation of the CH_3 group alone. Solid lines are the fits using eq 4. The proportion of chains contributing to the dynamics at each temperature is also indicated.

50% of the chains contribute to the dynamics and do not take part in interdigitation. This is inferred from the fact that the ratio of the interdigitated to noninterdigitated chains is also 50% as obtained from the geometry of the structure in a simple cubic lattice. With increasing temperature, more and more chains started contributing to the dynamics, and eventually at 380 K all the chains were dynamic. The AgOT results have been reported in ref 50. It may be noted that the superlattice melting temperature is ∼390 K and the feature observed at 380 K is similar to premelting.

A few interesting things are noticed in the case of the superlattice systems, AgDDT and AgODT. While quasielastic broadening is observed at room temperature in the case of AgDDT, no quasielastic broadening is seen in AgODT at room temperature. Partial melting of the chains is observed at different temperatures lower than 380 K in both systems. Most interestingly, in both systems, time-dependent partial melting is observed at 380 K. It is seen that, even at a constant temperature, the proportion of chains contributing to the dynamics increases slowly with time. It may be noted that, in the spectrometer used for the present study, measurements are done at a particular Q value at one time. The variation of EISF for AgDDT is shown in Figure 8. The arrows in the figure indicate the order in which the measurements were done at 380 K. Figure 9 shows the QENS spectra for AgDDT at different temperatures and Q values. For AgDDT at 380 K, initially about 65% of the chains were contributing to the dynamics, and afterward the contribution went up to 75%. No time-dependent changes were picked up by calorimetry in this sample. Thus, there appears to be a nearly thermoneutral event involving the alkyl chains at this temperature. This could also be (additionally) associated with cluster surface annealing as morphology changes are seen in

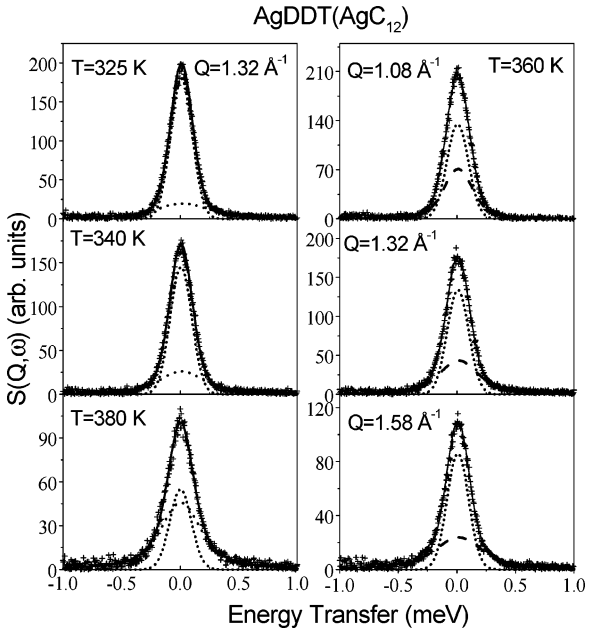

Figure 9. Typical QENS spectra and separated elastic (dotted) and quasielastic (dashed) components for AgDDT at 360 K for different Q values. Also shown are the spectra at typical $Q = 1.32$ Å^{-1} at different temperatures.

TABLE 1: Values of the Reorientation Time for Different Systems at Different Temperatures

		τ (ps)		
sample	temp (K)	isolated clusters	superlattice	layered thiolate
HT	300			
	325	4.7 ± 0.7	1.8 ± 0.3	
	340	3.5 ± 0.4	1.3 ± 0.3	3.6 ± 0.6
	360	2.8 ± 0.3	1.8 ± 0.3	4.1 ± 0.6
	380	2.3 ± 0.3	1.7 ± 0.3	7.3 ± 0.9
	400	2.1 ± 0.3	1.5 ± 0.3	9.9 ± 0.9
OT	300		5.2 ± 0.8	2.0 ± 0.3
	325	2.3 ± 0.4		
	340	1.7 ± 0.3	3.7 ± 0.5	1.8 ± 0.3
	360	1.5 ± 0.3	2.9 ± 0.6	3.5 ± 0.6
	380	1.4 ± 0.3	4.1 ± 0.8	3.7 ± 0.6
	400	1.2 ± 0.2		2.7 ± 0.5
DDT	300		4.3 ± 0.7	
	325	3.3 ± 0.4		
	340		4.0 ± 0.5	
	360		3.3 ± 0.4	
	380		time-dependent	
	400			3.8 ± 0.8
ODT	300			
	325			
	340	6.2 ± 0.8	3.5 ± 0.4	
	360	3.7 ± 0.6	3.0 ± 0.5	
	380	2.3 ± 0.4	time-dependent	2.9 ± 0.5
	400			2.6 ± 0.5

the clusters upon heating.[51] In the absence of additional studies, it is difficult to comment on this time-dependent event.

In AgODT[51] the dynamics was observed at and above 340 K. Fifty percent of the chains were dynamic at 340 K and 60% at 360 K, whereas the amount varied from about 70% to 90% at 380 K with time. For superlattice MPCs also, the model for the alkyl chain rotation is found to be uniaxial rotational diffusion. It was possible to describe the spectra at different temperatures and Q values assuming the same model. The obtained values of the reorientation times for different systems at different temperatures are given in Table 1. As mentioned above, in the superlattice system there are two types of chains,

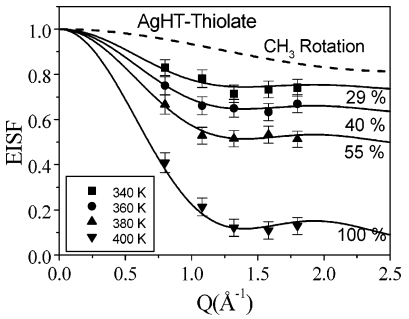

Figure 10. Variation of EISF with Q at different temperatures for AgHT−thiolate. The dashed line is the calculated EISF assuming rotation of the CH_3 group alone. Solid lines are the fits using eq 1. The proportion of the chains contributing to the dynamics at each temperature is also indicated.

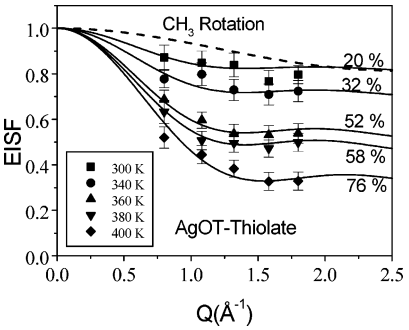

Figure 11. Variation of EISF with Q at different temperatures for AgOT−thiolate. The dashed line is the calculated EISF assuming rotation of the CH_3 group alone. Solid lines are the fits using eq 4. The proportion of the chains contributing to the dynamics at each temperature is also indicated.

interdigitated and noninterdigitated, which are expected to be dynamically different as the interdigitated ones are more strongly interacting among themselves compared to the others. However, what one observes in the QENS experiment is the average of all the protons, and when both types of chains contribute, it is not possible to separate these contributions. Therefore, the obtained reorientation time, τ, does not show systematic variation with temperature. At low temperature, the contribution may be only from the noninterdigitated ones. With an increase in temperature, others start contributing, and what is observed is the average of the two motions.

Layered Thiolates. To compare the results obtained from superlattice and isolated cluster MPCs (3D SAMs) with those obtained from corresponding planar systems, QENS experiments were carried out on layered thiolates known to represent the planar two-dimensional monolayers. In the category of layered thiolate systems, AgC_6 (AuHT), AgC_8 (AuOT), AgC_{12} (AgDDT), and AgC_{18} (AgODT) were studied. AgHT did not show quasielastic broadening up to 325 K. The variation of the experimentally obtained EISF (ratio of the elastic to quasielastic component) with Q is shown in Figure 10. Alkyl chains in these layered systems also undergo uniaxial rotational diffusion as seen from the figure. At 340 K about 30% of the chains are dynamic as obtained from the fit of the data using eq 4. Like MPCs, the component of mobile chains increases with temperature, and at 400 K, all chains are found to be dynamic.

However, in the case of AgOT−thiolate, although the quasielastic broadening is seen at room temperature, complete chain melting is not seen even at 400 K. The variation of EISF with Q is also shown in Figure 11 along with the calculated EISF for partial melting. Interestingly, in the case of the AgDDT−thiolate system, quasielastic broadening was observed

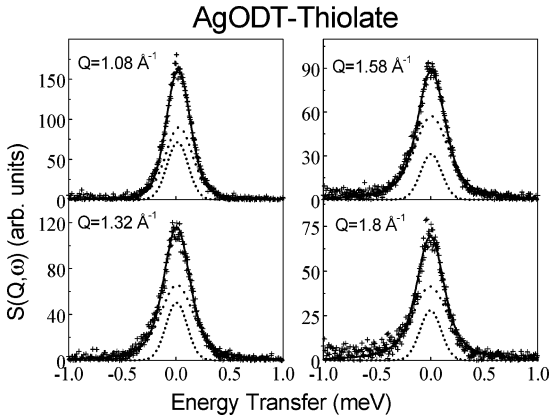

Figure 12. Typical QENS spectra and separated elastic (dotted) and quasielastic (dashed) components for AgODT−thiolate at different Q values and at $T = 400$ K.

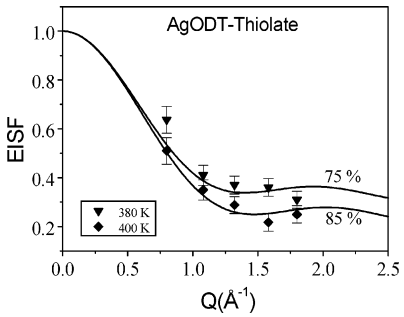

Figure 13. Variation of EISF with Q at different temperatures for AgODT−thiolate. Solid lines are the fits using eq 4.

only at $T = 400$ K. No quasielastic broadening is seen below 400 K. At $T = 400$ K, all chains were found to be dynamic.[50] In the case of the AgODT−thiolate system, no quasielastic broadening is seen below $T = 380$ K, while at 380 and 400 K, 75% and 85% chain melting, respectively, was observed. QENS spectra are shown in Figure 12 at different Q values for $T = 400$ K. The variations of EISF with Q at 380 and 400 K are shown in Figure 13. As per DSC results, the chain melting temperature is ∼400 K. The QENS data are consistent with this for the AgHT− and AgDDT−thiolate systems, whereas in the case of AgOT and AgODT, the alkyl chains perform restricted dynamics above 400 K, and finally the sample melts completely at 420 K. The chains in AgDDT and AgODT become mobile abruptly, whereas in others the mobility increases gradually.

Again uniaxial rotational diffusion describes the QENS data consistently. The obtained values of the reorientation times for different layered thiolate systems at different temperatures are given in Table 1.

IV. Discussion

In a typical metal cluster of 3−4 nm diameter, a few hundred monolayer chains are assembled. There could be a few tens of chains per plane of the cluster, and on each plane they form a pillar, especially in the case of longer chain lengths. Some chains can be disordered; this fraction in longer chain systems is too small to affect our measurements significantly. The alkyl chains are extended even in the dynamic state, making uniaxial rotation the principal dynamic motion.[50] The precessional motion of the chains is at least 5 times more energy intensive than the simple axial rotation as stated before. The alkyl chains in metal cluster solids are expected to have larger dynamical freedom than thiolates, as more space is available for the former in their structure.[50] As a result, the chains are expected to preserve uniaxial rotational freedom for an extended temperature window, while for thiolates, conformational disorder may set in after the collapse of the solid-state order. This collapse of the structure is likely to be instantaneous, while in the cluster solids, a more gradual evolution of dynamics is expected.

Data for isolated clusters suggest that, for smaller chain lengths, the dynamics evolves slowly and at 400 K all the chains are completely dynamic. In the case of MPCs above C_{12}, complete melting is observed above 340 K. This is in agreement with DSC and variable-temperature IR spectroscopy. DSC shows that, in systems below C_8, melting is featureless; however, for longer chain lengths, a sharp feature is observed at a temperature close to the corresponding chain melting temperature. This is evidenced by both IR[46] and neutron scattering[50,51] measurements. However, neutron scattering data clearly show that there are significant interchain interactions in the smaller chain length thiols, making the dynamics evolve only slowly, and a higher temperature is needed to achieve total rotational freedom. This occurs as there are conformational defects frozen into the system at RT, as evidenced in IR. The bend chains allow only hindered rotational motion. In the case of longer chain lengths, the alkyl chains are all-trans as a result of the increased van der Waals interaction. As a result, they form pillars on the lattice planes of the clusters. As these pillars are formed only in a smaller area, they collapse readily upon melting. There is a significant amount of free volume available in the solid for rotational motion, and consequently complete rotational dynamics is observed.

Uniaxial rotation is unlikely to result in the rotation of the whole chain from the methyl end to the S. This is evident from the NMR[35] and IR[38,39] data, which suggest that methylenes close to the cluster surface achieve rotational freedom only at much higher temperatures. As far as the S is concerned, it is likely to be rotationally frozen till the bulk chain melting transition. The decrease in the trans C−S intensity and the emergence of gauche C−S indicate rapid conformational changes around this temperature. Thus, only above the bulk melting temperature, complete uniaxial rotation of the whole chain is expected. This is true in superlattice solids also where the dynamics evolves slowly. Thus, as the temperature increases, more methylenes participate in the rotations, and above bulk melting the entire chain is rotationally free.

It is necessary to clarify the meaning of fractional dynamics. We suggest this to mean that only a fraction of the alkyl chains are undergoing motions. In the case of monolayers forming pillars on the surface of the planes, it is very much likely that the chains on the edges of the monolayer assembly (or the free chains not part of the assembly) will become dynamic first, as they are the ones with less interchain interactions. As they get detached from the bulk monolayer assembly, they acquire dynamical freedom. It would be easier for the shorter chain monolayers to detach from the assembly earlier than the longer chains. In the longest chain systems, the chains are all-trans and completely extended, and as a result detachment may result in a free chain, which is free to be dynamically active. For the intermediate chain lengths, where conformational disorder can exist, detachment from the assembly could be more energy intensive. It has been shown in the previous section that gradual evolution of melting along the chain is not probable as the behavior of the EISF in AuHT, AgHT, and layered thiolate systems is not explainable by the end CH_3 motion and is expected to be dynamic first within a whole chain.

The fact that the interchain distance is smaller than the van der Waals diameter (a chain radius of 2.1 Å is found in MPCs, whereas the distance between chains in planar monolayers is ~5 Å) implies strong interaction between the chains which can only be interpreted in terms of the closer packing of chains in the form of pillars on the cluster surface. As temperature increases, some chains are likely to detach from the pillarlike assembly, contributing to the dynamics as mentioned above. However, the last few methylenes (closer to the cluster core) may not have the required space to avail free rotation as the cluster surface is completely covered with thiolate chains.

In the planar thiolates, the motion continues to be uniaxial rotation, but as temperature increases, chains begin to manifest conformational disorder. The melting behavior seen in the systems is in accordance with the DSC data in the literature[22] and our own studies (data presented in Supporting Information Figure 1). All the systems begin to show melting around 398 K, and the data show very little change with chain length. Melting of the alkyl chains was studied by variable-temperature IR spectroscopy. The temperature-dependent IR spectra of AgOT and AgDDT are shown in Supporting Information Figures 2 and 3, respectively. In both systems, the symmetric (d_+) and asymmetric (d_-) methylene modes as well as the progression modes show a drastic change at the melting temperature. Except in AgOT, the progression bands disappear, corresponding to complete melting. In the case of AgOT, however, the progression bands do not disappear completely, corresponding to persistent conformational order even after 398 K. However, they do disappear at 420 K, consistent with the neutron data at this temperature. The presence of defects is evident in the IR spectra of AgHT and AgOT at room temperature. End gauche defects in the methylene chains are manifested in OT as a peak at 1343 cm^{-1}. Upon melting, the IR spectra in all the cases manifest peaks at 1297 cm^{-1} due to W(g−t−g) kink defects.[56,57] Upon melting, the C−S(g) is more pronounced in AgOT and the conformation is preserved upon cooling back to room temperature. All of these collectively indicate that this system is distinctly different. A similar observation is applicable to the layered AgODT−thiolate system also.

Lower chain thiolate AgHT shows a higher reorientation time at higher temperatures. The reorientation time increases from 3.6 to 9.9 ps as the temperature increases from 340 to 400 K. Only lower reorientation times are observed in longer chain length thiolates. This would mean that, in AgHT after melting, the chains possibly deform, resulting in conformational defects, which lead to hindered rotations and higher reorientation times. This is more likely in the case of shorter chains as interchain interactions are weaker, allowing chain deformation. The IR data agree with this interpretation.

Taken together, the data confirm that the alkyl chains are organized like bundles on the cluster planes, consistent with MD studies,[33,34] and this prevents buckling at high temperatures. As a result, uniaxial motion continues to persist at higher temperatures in the case of cluster monolayers. For planar thiolates, the interchain interactions are uniform throughout the solid and no pillar formation exists, which makes it possible for the chains to buckle at higher temperatures. It appears that there is a partially ordered phase in layered AgOT−thiolate persisting above the DSC melting transition, with local order at least in the lower parts of the thiolate chain (toward S), which required still higher temperatures for complete melting. This appears to correspond to the mesogenic behavior observed in thiolates.[20] Optical investigations have found such a phase existing well beyond the onset of melting. It may be noted that the amorphous phase is seen in AgOT only above 480 K, whereas in longer chain thiolates such as AgODT this happens above 448 K.[20] It is important to mention that the micellar−amorphous transition mentioned above is not seen in DSC. The presence of mesophases prevents uniaxial rotation for the whole chain. Thus, it appears that the rotational dynamics in thiolates is similar to that in monolayers on cluster systems but restricted dynamics due to buckling occurs at still higher temperatures. This is possible as interchain distances appear to be larger in thiolates than in the case of cluster monolayers. Thus, a distinct difference in the high-temperature dynamics is a result of the difference in the molecular architecture of the two systems.

We add that the kind of packing might be similar for longer and shorter chains. However, it is easier for the chains to detach from the columns of alkyl chain assemblies and participate in the rotational dynamics. By this process, there will be a larger fraction of the shorter chains undergoing dynamics at any given temperature than the longer chains.

In monolayer-protected metal cluster solids, the conformational order of the alkyl chains depends on two parameters, the cluster core size and the chain length of the monolayer. When the chain is long, interchain interactions are large. This makes the monolayers stand up to give an all-trans structure, leading to a precise melting temperature. When the size of the cluster core is large, the interchain interactions of a large number of chains are possible as the number of chains on a given plane is high, making the chains erect. For a given kind of cluster core size, a smaller chain length will reduce the conformational order. Thus, in the systems investigated, we have three extremes where conformational disorder, alkyl chain order, and a regular superlattice exist. When the chain length is inadequate, alkyl chains may not form the pillarlike structure. In longer chain lengths, the pillar formation is complete, but if the cluster core dimension is nonuniform, isolated cluster structure dominates. The occurrence of uniformity in core dimension along with alkyl chain order leads to the formation of regular superlattices as in the case of silver.

V. Conclusions

Our studies, encompassing a range of chemical systems, have given a consistent picture of the dynamics of alkyl chain assembles in isolated monolayer-protected clusters, interdigitated metal cluster superlattices, and planar thiolates. The dynamics in all these systems can be adequately described by uniaxial rotation. While the chains acquire dynamical freedom slowly in the cluster systems, bulk melting suddenly brings about rotational freedom in planar thiolates. The chains of longer chain monolayers are rotationally frozen in cluster systems at room temperature, and no rotator phase exists. The data imply strong interactions between the chains making the monolayers assemble as pillars on the cluster surfaces, and the pillars interdigitate, forming superlattices. It is also clear that, even after bulk melting, in some of the thiolates, partial order exists which prevents complete free rotation. We understand the differences in dynamics in these systems in terms of the variation in the space available for the monolayers. In thiolates, the chains can also collapse after melting, leading to restricted rotational freedom. These conformational defects are also seen in the variable-temperature IR spectroscopy.

Acknowledgment. T.P. acknowledges financial support from the Inter University Consortium for DAE Facilities for funding a research scheme. His monolayer-protected cluster program

has been supported by the Department of Science and Technology and Council of Scientific and Industrial Research, Government of India. Equipment support by the Nanoscience and Nanotechnology initiative is acknowledged.

Supporting Information Available: DSC and variable-temperature IR data of thiolates (PDF). This information is available free of charge via the Internet at http://pubs.acs.org.

References and Notes

(1) Yamamoto, Y.; Nishihara, H.; Aramaki, K. *J. Electrochem. Soc*. **1993**, *140*, 436.
(2) Ehler, T. T.; Malamberg, N.; Carron, K.; Sullivan, B. P.; Nee, J. *J. Phys. Chem. B* **1997**, *101*, 3174.
(3) Brust, M.; Walker, M.; Bethell, D.; Schiffrin, D. J.; Whyman, R. *J. Chem. Soc., Chem. Commun.* **1994**, 801.
(4) Kepley, L. J.; Crooks, R. M.; Ricco, A. J. *Anal. Chem.* **1992**, *64*, 3191.
(5) Hostetler, M. J.; Green, S. J.; Stokes, J. J.; Murray, R. W. *J. Am. Chem. Soc.* **1996**, *118*, 4212.
(6) Häussling, L.; Michel, B.; Ringsdorf, H.; Rohrer, H. *Angew. Chem., Int. Ed. Engl.* **1991**, *30*, 569.
(7) Frostman, L. M.; Bader, M. M.; Ward, M. D. *Langmuir* **1994**, *10*, 576.
(8) Hostetler, M. J.; Murray, R. W. *Curr. Opin. Colloid Interface Sci.* **1997**, *2*, 42; Sandhyarani, N.; Pradeep, T. *Int. Rev. Phys. Chem*. **2003**, *22*, 221−262; Pradeep, T.; Sandhyarani, N. *Pure Appl. Chem.* **2002**, *74*, 1593−1607.
(9) Ulman, A. *Adv. Mater*. **1991**, *3*, 298.
(10) Nuzzo, R. G.; Allara, D. L. *J. Am. Chem. Soc.* **1983**, *105*, 4481.
(11) Nuzzo, R. G.; Dubois, L.. H.; Allara, D. L. *J. Am. Chem. Soc*. **1990**, *112*, 558.
(12) Laibinis, P. E.; Whitesides, G. M.; Allara, D. L.; Tao, Y. T.; Parikh, A. N.; Nuzzo, R. G. *J. Am. Chem. Soc.* **1991**, *113*, 7152.
(13) Chidsey, C. E. D.; Liu, G.-Y.; Rowntree, P.; Scoles, G. *J. Chem. Phys.* **1991**, *94*, 8493.
(14) Camillone, N., III; Chidsey, C. E. D.; Liu, G.-Y.; Putvinski, T. M.; Scoles, G. *J. Chem. Phys.* **1991**, *94*, 8493.
(15) Camillone, N.; Eisenberger, P.; Leung, T. Y. B.; Schwartz, P.; Scoles, G.; Poirier, G. E.; Tarlov, M. J. *J. Chem. Phys.* **1994**, *12*, 11031.
(16) Poirier, G. E. *J. Vac. Sci. Technol., B* **1996**, *14*, 1453.
(17) Biebuyck, H. A.; Bain, C. D.; Whitesides, G. M. *Langmuir* **1994**, *10*, 1825.
(18) Dance, I. G.; Fisher, K. J.; Herath Banda, R. M.; Scudder, M. L. *Inorg. Chem*. **1991**, *30*, 183.
(19) Parikh, A. N.; Gillmor, S. D.; Beers, J. D.; Beardmore, K. M.; Cutts, R. W.; Swanson, B. I. *J. Phys. Chem. B* **1999**, *103*, 2850.
(20) Baena, M. J.; Espinet, P.; Lequerica, M. C.; Levelut, A. M. *J. Am. Chem. Soc*. **1992**, *114*, 4182.
(21) Fijolek, H. G.; Grohal, J. R.; Sample, J. L.; Natan, M. J. *Inorg. Chem*. **1997**, *36*, 622.
(22) Bensebaa, F.; Ellis, T. H.; Kruus, E.; Viocu, R.; Zhou, Y. *Langmuir* **1998**, *14*, 6579.
(23) Kruger, D.; Rousseau, R.; Fuchs, H.; Marx, D. *Angew. Chem., Int. Ed*. **2003**, *42*, 2251.
(24) Wang, B.; Wang, H. Q.; Li, H. X.; Zeng, C. G.; Hou, J. G.; Xiao, X. D. *Phys. Rev. B* **2001**, *63*, Article No. 035403.
(25) Thomas, P. J.; Kulkami, G. U.; Rao, C. N. R. *Chem. Phys. Lett*. **2000**, *321*, 163.
(26) Hasan, M.; Bethell, D.; Brust, M. *J. Am. Chem. Soc.* **2002**, *124*, 1132.
(27) Hautman, J.; Klein, M. *J. Chem. Phys.* **1990**, *93*, 7483.
(28) Mar, W.; Klein, M. L. *Langmuir* **1994**, *10*, 188.
(29) Hautman, J.; Klein, M. *J. Chem. Phys.* **1989**, *91*, 4994.
(30) Taut, C.; Pertsin, A. J.; Grunze, M. *Langmuir* **1996**, *12*, 3481.
(31) Bhatia, R.; Garrison, B. J. *Langmuir* **1997**, *13*, 765.
(32) Sadreev, A. F.; Sukhinin, Y. V. *J. Chem. Phys.* **1997**, *107*, 2643.
(33) Luedtke, W. D.; Landman, U. *J. Phys. Chem.* **1996**, *100*, 13323.
(34) Luedtke, W. D.; Landman, U. *J. Phys. Chem. B* **1998**, *102*, 6566.
(35) Terril, R. H.; Postlethwaite, T. A.; Chen, C.-H.; Poon, C.-D.; Terzis, A.; Chen, A.; Hutchison, J. E.; Clark, M. R.; Wignall, G.; Londono, J. D.; Superfine, R.; Falvo, M.; Johnson, C. S.; Samulski, E. T., Jr.; Murray, R. W. *J. Am. Chem. Soc.* **1995**, *117*, 12537.
(36) Nuzzo, R. G.; Dubois, L.. H.; Allara, D. L. *J. Am. Chem. Soc.* **1990**, *112*, 558.
(37) Laibinis, P. E.; Whitesides, G. M.; Allara, D. L.; Tao, Y. T.; Parikh, A. N.; Nuzzo, R. G. *J. Am. Chem. Soc*. **1991**, *113*, 7152.
(38) Terril, R. H.; Tanzer, T. A.; Bohn, P. W. *Langmuir* **1998**, *14*, 845.
(39) Badia, A.; Denners, L.; Dickinson, L.; Morin, F. G.; Lennox, R. B.; Reven, L. *J. Am. Chem. Soc*. **1997**, *119*, 11104.
(40) Chechik, V.; Schonher, H.; Vansco, G. J.; Stirling, C. J. M. *Langmuir* **1998**, *11*, 3003.
(41) Poirier, G. E. *Langmuir* **1999**, *15*, 1167.
(42) Venkataramanan, M.; Pradeep, T. *Anal. Chem*. **2000**, *72*, 5852.
(43) Badia, A.; Singh, S.; Demers, L.; Cuccia, L.; Brown, G. R.; Lennox, R. B. *Chem.—Eur. J.* **1996**, *2*, 359.
(44) Badia, A.; Cuccia, L.; Demers, L.; Morin, F.; Lennox, R. B. *J. Am. Chem. Soc*. **1997**, *119*, 2682.
(45) Badia, A.; Gao, W.; Singh, S.; Demers, L.; Cuccia, L.; Reven, L. *Langmuir* **1996**, *12*, 1262.
(46) Sandhyarani, N.; Antony, M. P.; Panneer Selvam, G.; Pradeep, T. *J. Chem. Phys.* **2000**, *113*, 9794.
(47) Snyder, R. G. *J. Mol. Spectrosc.* **1961**, *7*, 116.
(48) Dubois, L. H.; Nuzzo, R. G. *Annu. Rev. Phys. Chem.* **1992**, *43*, 437.
(49) Bee, M. *Quasielastic Neutron Scattering*; Adam-Hilger: Bristol, 1988.
(50) Mitra, S.; Binoj Nair.; Pradeep, T.; Goyal, P. S.; Mukhopadhyay, R. *J. Phys. Chem. B* **2002**, *106*, 3960.
(51) Mukhopadhyay, R.; Mitra, S.; Pradeep, T.; Tsukushi, T.; Ikeda, S. *J. Chem. Phys*. **2003**, *118*, 4614.
(52) Mukhopadhyay, R.; Mitra, S.; Tsukushi, I.; Ikeda, S.; Pradeep, T. *Chem. Phys*. **2003**, *292*, 223.
(53) Sandhyarani, N.; Resmi, M. R.; Unnikrishnan, R.; Vidyasagar, K.; Ma, S.; Antony, M. P.; Selvam, G. P.; Visalakshi, V.; Chandrakumar, N.; Pandian, K.; Tao, Y.-T.; Pradeep, T. *Chem. Mater*. **2000**, *12*, 104.
(54) Sandhyarani, N.; Pradeep, T. *J. Mater. Chem*. **2001**, *11*, 1294.
(55) Mukhopadhyay, R.; Mitra, S.; Paranjpe, S. K.; Dasannacharya, B. A. *Nucl. Instrum. Methods, A* **2001**, *474*, 55.
(56) Maroncelli, M.; Qi, S. P.; Strauss, H. L.; Synder, R. G. *J. Am. Chem. Soc*. **1982**, *104*, 6237.
(57) Venkataraman, N. V.; Vasudevan, S. *J. Phys. Chem. B* **2001**, *105*, 7639.